Speeds of sound in n-pentane at temperatures from (233.50 to 473.15) K at pressures up to 390 MPa

Christian W. Scholz[1] (c.scholz@thermo.rub.de)***, Yolanda Sanchez-Vicente***[2] (y.sanchez-vicente@imperial.ac.uk)***, Tana Tananilgul***[2] (tana.tananilgul16@imperial.ac.uk)***, Monika Thol***[1] (m.thol@thermo.rub.de)***, J. P. Martin Trusler***[2] (m.trusler@imperial.ac.uk)***, Markus Richter***[3,*] (m.richter@mb.tu-chemnitz.de)

[1]*Thermodynamics, Ruhr University Bochum, 44780 Bochum, Germany*

[2]*Department of Chemical Engineering, Imperial College London, South Kensington Campus, London SW7 2AZ, United Kingdom*

[3]*Applied Thermodynamics, Chemnitz University of Technology, 09107 Chemnitz, Germany*

ABSTRACT

We report speeds of sound in n-pentane measured using two similar apparatuses, located at Ruhr University Bochum (RUB) and Imperial College London (ICL), covering different ranges of temperature and pressure. At RUB, measurements were conducted at temperatures from (233.50 to 353.20) K with pressures up to 20 MPa, while temperatures from (263.15 to 473.15) K with pressures up to 390 MPa were covered at ICL. Accounting for the uncertainties in temperature, pressure, path-length calibration, and pulse timing, the relative expanded combined uncertainty ($k = 2$) in the speed of sound varied from 0.015% to 0.18% over the whole region investigated. Nevertheless, small differences averaging at 0.13% are found between the two data sets in the region of overlap. The experimental data reported in this work have been partly used in the development of a new fundamental equation of state for n-pentane.

Keywords: High pressure; Pulse-echo technique; n-Pentane; Speed of sound

* Corresponding author

1 INTRODUCTION

The alkane n-pentane has a significance in various industrial applications since it is used as a working fluid in geothermal power plants[1] and refrigeration cycles, where it is known as refrigerant R601. Moreover, n-pentane can be used in the foaming of insulating materials,[2] as solvent and eluent in the food industry[3] and as a reaction medium for polymerization.[4] n-Pentane is a component in natural gas, liquefied petroleum gas and other hydrocarbon fuels and is, therefore, an essential component in mixture models applied to such fuels.

A fundamental equation of state for n-pentane was developed by Span and Wagner[5] and is currently being replaced by a new fundamental equation of state, being developed at Ruhr University Bochum by Thol et al.[6] as already implemented in REFPROP 10.0[7] and TREND 4.0.[8] Among other thermodynamic properties, the speed of sound data sets of El Hawary et al.[9] (liquid phase), Ewing et al.[10] (gas phase) and Chávez et al.[11] (saturation line) were considered as primary data for the development of this equation, as well as the data investigated at RUB within the scope of the present work. The distribution of these data is presented in Figure 1, together with the state points investigated in this work at ICL as well as further data from literature. A literature review of the available experimental (p, c, T) data, including the number of points as well as the temperature and pressure ranges, is summarized in Table 1. Even though several speed of sound data sets are available in literature, some of the data sets differ significantly from each other and, thus, complicate the development of a reliable equation of state. The present study was initiated with the objective to increase the amount and scope of the available data for use in the development of the equation of state by Thol et al.[6] El Hawary et al.[9] completed their experimental data set at Helmut-Schmidt-University (HSU) Hamburg simultaneously but completely independent from our present measurements. The apparatuses at RUB and HSU are both designed for reliable speed of sound measurements even at low pressures and can be used to clarify the data situation by

independent and overlapping measurements. Our work also includes extensive results obtained with an apparatus at ICL, optimised for high-pressure and high-temperature measurements, which extends the ranges of pressure and temperature up to 390 MPa and 473.15 K, respectively.

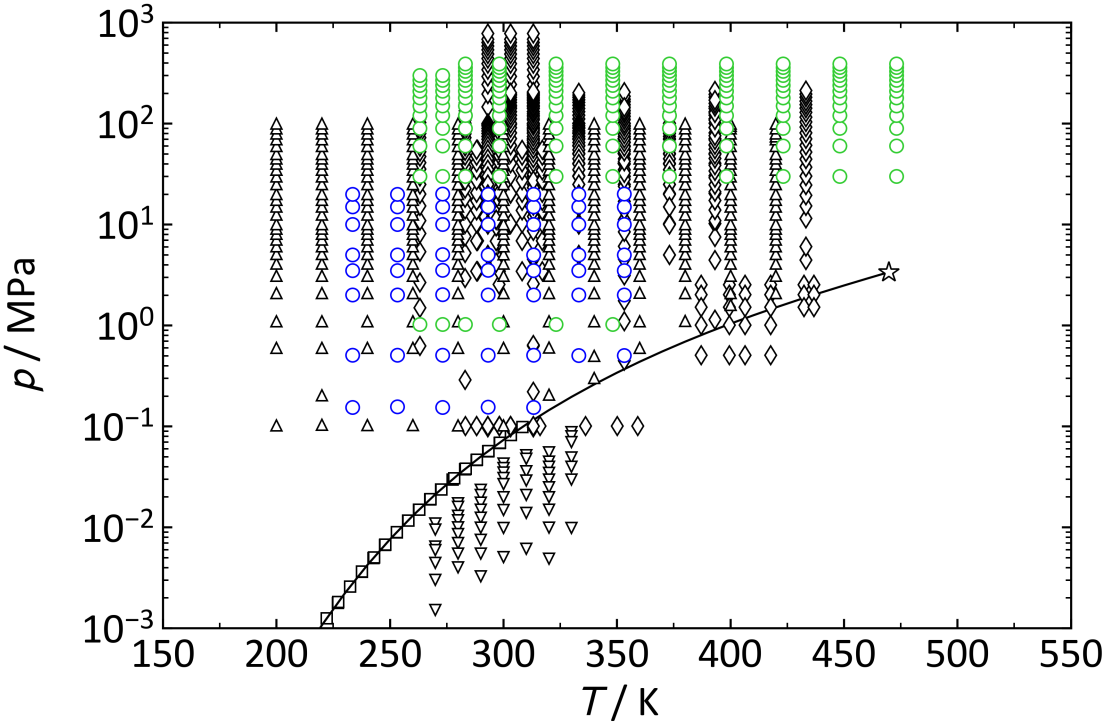

Figure 1. Selection of experimental (p, c, T) data for n-pentane from literature and (p, T) state points investigated in the present work shown in a pressure vs. temperature phase diagram. ○, this work at RUB; ○, this work at ICL; △, El Hawary et al.;[9] ▽, Ewing et al.;[10] □, Chávez et al.[11]; ◇, further data from literature (see Table 1); —, phase boundary and ☆, critical point, calculated with the equation of state by Thol et al.[6]

Table 1. Review of speed of sound measurements in n-pentane.

Author	Year	Points	T / K	p / MPa	Phase [a]
Belinskii and Ikramov[12]	1973	48	293 – 313	0.1 – 785	liquid
Benson and Handa[13]	1981	1	298.14	0.1013	liquid
Chávez et al.[11]	1982	44	206 – 308	0.0003 – 0.1	SATL
Dalai et al.[14]	2012	1	313.16	0.1013	liquid
Ding et al.[15]	1997	200	293 – 373	5.0 – 100	liquid
Dixon and Greenwood[16]	1924	4	316 – 360	0.1013	gas
El Hawary et al.[9]	2019	319	200 – 420	100	liquid
Ewing et al.[10]	1989	58	270 – 330	0.001 – 0.1	gas
Handa et al.[17]	1981	1	298.14	0.1013	liquid
Ismagilov et al.[18]	1982	26	387 – 437	0.5 – 2.5	liquid
Kiryakov and Otpushchennikov[19]	1971	57	303 – 334	10.1 – 203	liquid
Lainez et al.[20]	1990	220	263 – 434	0.2 – 213	liquid
Melnikov et al.[21]	1988	10	153 – 434	0.00001 – 2	SATL
Nath[22]	1997	1	293.15	0.1013	liquid
Nath[23]	1998	1	298.15	0.1013	liquid
Nath[24]	2000	1	303.15	0.1013	liquid
Nath[25]	2002	1	288.15	0.1013	liquid
Neruchev et al.[26]	2005	35	193 – 470	0.0001 – 4	SATL
Otpushchennikov et al.[27]	1974	35	303 – 394	0.1 – 203	liquid
Rai et al.[28]	1989	1	298.14	0.1013	liquid
Richardson[29]	1958	11	288.54	3.4 – 56	liquid
Richardson and Tait[30]	1957	44	288 – 318	3.4 – 56	liquid
Sachdeva and Nanda[31]	1981	5	283 – 304	0.1013	liquid
Schaaffs[32]	1944	1	293.14	0.1013	liquid
Scholz et al. (*this work at RUB*)	2020	54	233 – 353	0.15 – 20	liquid
Scholz et al. (*this work at ICL*)	2020	143	263 – 473	1.02 – 390	liquid
Shukla et al.[33]	2008	1	298.15	0.1013	liquid
Singh et al.[34]	2012	3	293 – 304	0.1013	liquid
Swanson[35]	1934	5	296.74	4.2 – 12	liquid
Vyas[36]	2004	1	298.15	0.1013	liquid
Weissler and Del Grosso[37]	1950	2	293 – 304	0.1013	liquid

[a] SATL denotes saturated liquid states.

2 EXPERIMENTAL SECTION

2.1 Apparatus description. The work we report here was carried out using two different apparatuses, located at Ruhr University Bochum (RUB) and Imperial College London (ICL), employing the same principle to measure sound speed, which is the double-path pulse-echo technique. In this method, a piezoelectric disc transducer is mounted perpendicular to the axis of a cylindrical cell closed at each end by plane reflectors. The transducer is located at unequal distances L_1 and L_2 from the reflectors. To initiate a measurement, the transducer is excited by a tone burst, causing ultrasonic pulses to propagate into the fluid on both sides. These pulses are reflected at the end plates and return to the transducer, thereby generating an electronic signal that can be captured with a digital oscilloscope. Because of the unequal path lengths, the two returning echoes arrive at different times. The time difference Δt_{echo} between the two echoes is determined from the measured signal and the speed of sound c is determined from the relation:

$$c = \frac{2\left(L_2 - L_1\right)}{\Delta t_{\text{echo}} + \tau} \tag{1}$$

This equation incorporates a small correction τ to account for diffraction, calculated according to Harris,[38] that evaluates the time difference between the ideal plane-wave and the real case. For the measurements in n-pentane conducted in the scope of this work, $\tau/\Delta t_{\text{echo}}$ varies between (0.001 and 0.031)%. In both apparatuses, the nominal path lengths were L_1 = 20 mm and L_2 = 30 mm. The actual path length difference $\Delta L = L_2 - L_1$ was represented in this work by means of the following equation:

$$\Delta L\left(T, p\right) = \Delta L_0 \left[1 + \alpha\left(T - T_0\right) - \frac{\beta}{3}\left(p - p_0\right)\right] \tag{2}$$

Here, ΔL_0 is the path-length difference at a reference temperature T_0 and reference pressure p_0, α is the mean value of the isobaric expansivity of the cell at pressure p_0 over the temperature interval [T_0, T], and β is the mean compressibility of the cell at temperature T over the pressure interval

[p_0, p]. In the following, the apparatuses of the two laboratories and the calibration of the path lengths will be described in brief.

2.1.1 Apparatus at Ruhr University Bochum. The speed of sound apparatus used at Ruhr University Bochum was based on the design of Meier and Kabelac,[39] set up according to Gedanitz et al.[40] and further improved by Wegge[41] and Wegge et al.,[42] where the apparatus is also described in detail. In this apparatus, the piezoelectric transducer was an x-cut quartz crystal. It was excited by a 30-cycle sinusoidal burst at a carrier frequency of 8 MHz, modulated by a half-cycle sin² function, generated by a waveform generator (Agilent, model 33220A). The signal developed across the transducer was captured with a digital oscilloscope (Agilent, model MS6032A), which was set to average the waveform from 16 consecutive pulses. For the sake of enhancing the signal-to-noise ratio, we applied a bandpass filter to the averaged data, based on a Fast-Fourier-Transform with a bandwidth of 1.6 MHz; zero padding in the frequency domain improved the time resolution of the echoes. The time difference Δt_{echo} between the first and second echo was then computed on basis of the processed data according to the algorithm described by Dubberke et al.[43]

The acoustic sensor was housed in a stainless-steel pressure vessel, and the connection between the sensor inside the pressure vessel and the electronic devices outside was realised by implementation of a glass feed-through. In order to ensure stable temperature conditions, the pressure vessel was completely immersed into a calibration bath thermostat (Fluke, model 7060). The thermostat was filled with a mixture of ethylene glycol and water, so that a temperature range from (233 to 353) K could be covered. The temperature was measured with a long stem 25 Ω standard platinum resistance thermometer (SPRT, Rosemount Aerospace, model 162CE) that was calibrated on the ITS-90 and connected to a direct current thermometry bridge (Isotech, model TTI-2). The standard uncertainty for temperature was $u(T)$ = 0.004 K. Pressures were measured

using two vibrating-quartz-crystal pressure transducers (Paroscientific, models 1000-500A and 1000-6K) with different pressure ranges. In order to avoid contamination of the pressure transducers with the liquid sample in the measuring cell, a differential pressure indicator (Rosemount, model 3051) was used to separate the measuring cell and the pressure measuring circuit. To improve stability, the pressure transducers and differential pressure indicator were also thermostated by a circulation bath thermostat. The standard uncertainty for pressure was $u(p)$ = 0.0012 MPa.

At RUB, the reference conditions in eq 2 were T_0 = 293.15 K and p_0 = 0.1 MPa, and the mean expansivity was determined by integration of values for the differential thermal expansion of stainless steel 1.4571 and represented by the following polynomial, in which a_0 was obtained from the calibration, and a_1 to a_4 were fixed at the values given by Meier:[44]

$$10^6 \alpha / \mathrm{K}^{-1} = \sum_0^4 \frac{a_i}{(i+1)} \cdot \left(\frac{T - T_0}{T_0} \right)^i \tag{3}$$

The coefficients of eq 3 are given in Table 2 and, for the purpose of the uncertainty analysis, the relative standard uncertainty of α was estimated to be 5 %. The mean isothermal compressibility β was obtained from material-property data[45] as follows

$$\beta = (1 - 2\nu)/E = (1 - 2\nu) \left[\sum_0^1 b_i (T / \mathrm{K})^i \right]^{-1} \tag{4}$$

where E is Young's modulus, and ν = 0.3 is Poisson's ratio, assumed independent temperature. The coefficients of eq 4 are given in Table 3.

Table 2. Coefficients of eqs 3 (RUB) and 5 (ICL) for the mean thermal expansivity α of the stainless steel 1.4571 cell at RUB and the Invar cell at ICL (see section 2.1.2).

	a_0	a_1	a_2	a_3	a_4
RUB	8.368	5.08059	- 3.7448	1.8672	$- 3.4148 \cdot 10^{-1}$
ICL	1.650	$8.552 \cdot 10^{-4}$	$2.941 \cdot 10^{-5}$	$4.397 \cdot 10^{-8}$	-

Table 3. Coefficients of eqs 4 (RUB) and 6 (ICL) for the mean isothermal compressibility β of the stainless steel 1.4571 cell at RUB and the Invar cell at ICL (see section 2.1.2).

	b_0	b_1	b_2
RUB	219.720	- 0.080	-
ICL	$1.061 \cdot 10^{2}$	$3.115 \cdot 10^{-2}$	$3.722 \cdot 10^{-4}$

To determine the pathlength difference ΔL_0 at the reference state and the scale parameter a_0 in eq 3 for the mean thermal expansion coefficient, calibration measurements of Δt_{echo} were carried out in high-purity water at nine state points at T = (274.15, 278.15, 283.15, 293.15, 303.15, 313.15, 333.15, 343.15 and 353.15) K and ambient pressure. The speeds of sound at these state points were evaluated from the IAPWS-95 equation of state of Wagner and Pruß,[46] and the parameters ΔL_0 and a_0 were regressed using eqs 1, 2 and 3. In Figure 2, we compare the resulting speeds of sound at all nine state points with the IAPWS-95 formulation and with experimental data reported by Del Grosso and Mader[47] and Fujii and Masui.[48] All experimental speed of sound data fall within the uncertainty of the equation of state, which was estimated by Wagner and Pruß to be 0.005 % in this restricted temperature range.

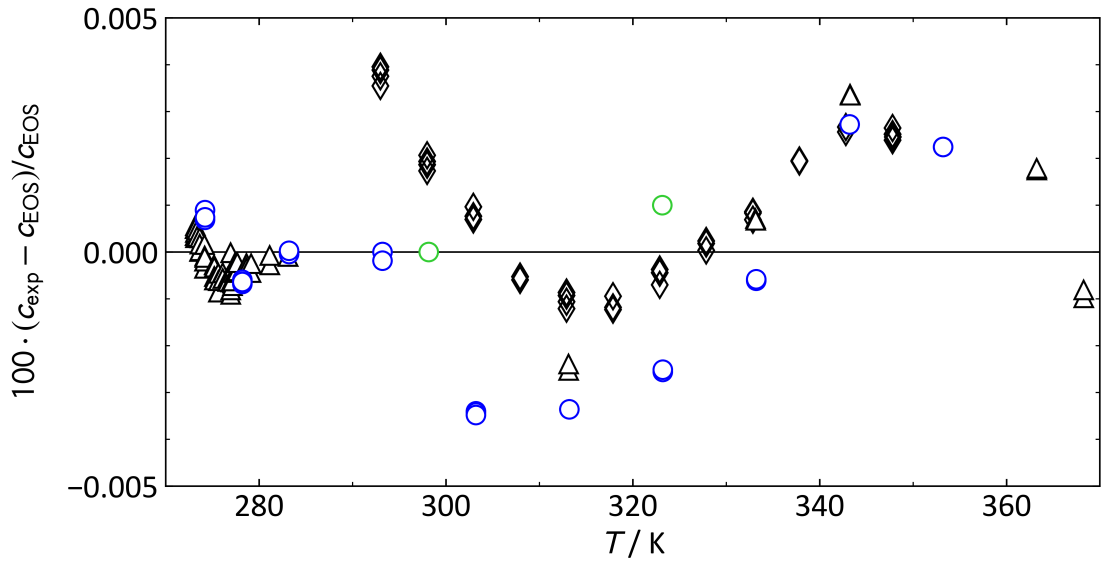

Figure 2. Relative deviations of experimental speeds of sound in pure water c_{exp} from values c_{EOS} calculated with the equation of state of Wagner and Pruß[46] plotted against temperature. Except where noted, the pressure is 0.1 MPa. ○, this work (RUB); ○, this work (ICL) at p = 1.0 MPa; △, Del Grosso and Mader;[47] ◇, Fujii and Masui.[48] The EOS is represented by the zero line and has a relative expanded uncertainty of 0.005 % at 95 % probability.

2.1.2 Apparatus at Imperial College London. The apparatus at Imperial College London is based on that described in detail in previous papers.[49-51] However, a new ultrasonic cell fabricated from Invar 36 nickel-iron alloy (36 mass% Ni + 64 mass% Fe) was used; this cell is identical to that described recently by Al Ghafri et al.[52] The piezoelectric transducer was a 5 MHz thickness-mode lead zirconate titanate piezoceramic disc (Piezo Technologies, Type K350 10 mm diameter) with fired-on gold electrodes. This was excited by a five-cycle tone burst at a carrier frequency of 5 MHz, generated by a function generator (Agilent, model 33120), and the returning signal was captured with a digital oscilloscope (Agilent, DSO6012A). The time difference Δt_{echo} between the returning echoes was determined by the algorithm described by Ball and Trusler.[46]

The ultrasonic cell was mounted within a pressure vessel, rated for a maximum working pressure of 400 MPa, which was immersed in a thermostat bath (Fluke model 6020) filled with silicone oil.

In order to permit operation at temperatures below about 313 K, a copper heat exchanger was immersed in the silicone oil through which chilled ethanol was circulated by an external circulating refrigerated bath. The pressure vessel was connected to a system of valves and a manual syringe pump which permitted pressures of up to 400 MPa to be generated. A single transducer (Honeywell model TJE/60000) located in the external pipework was used to measure the pressure. This transducer was calibrated as described by Tay and Trusler[51] and zeroed under vacuum immediately prior to the measurements on each isotherm. The temperature was measured by means of a platinum resistance thermometer (Fluke model 5615) calibrated on ITS 90. The resistance of this thermometer was measured at the temperature of the triple point of water immediately prior to this work. The standard uncertainty of the temperature was $u(T) = 0.015$ K, while that of the pressure was the larger of $0.0006 \cdot p$ and 0.05 MPa.

At ICL, the reference condition in eq 2 were $T_0 = 298.15$ K and $p_0 = 1.0$ MPa. The integral thermal expansion of the Invar was measured at the UK National Physical Laboratory, using a Linseis dilatometer relative to a fused-silica reference sample. The sample used for this was a 50 mm long bar of 3 mm x 3 mm rectangular cross-section cut (by means of electrical discharge machining) from the same billet used in the fabrication of the ultrasonic cell. The mean thermal expansion over the interval $[T_0, T]$ was correlated with the following equation

$$10^6 \alpha / \mathrm{K}^{-1} = \sum_0^3 a_i \left(T - 298.15\right)^i \tag{5}$$

The coefficients of eq 5 are given in Table 2. The expanded uncertainty at 95% confidence was reported to be $0.2 \cdot 10^{-6}$ K^{-1}. Compared with the expansion data reported by Tanji[53] for an Invar alloy containing 35.5 mass% Ni, the present results are approximately $0.6 \cdot 10^{-6}$ K^{-1} greater. The isothermal compressibility was obtained from $\beta = 1/K$, where K is the isothermal bulk modulus, which was taken from Hausch and Warlimont,[54] who reported ultrasonic measurements with a

relative uncertainty of 1 % carried out on a single-crystal sample at temperatures between 255 K and 500 K. These data were represented as a function of temperature as follows:

$$K \,/\, \mathrm{GPa} = \sum_{0}^{2} b_i (T \,/\, \mathrm{K} - 298.15)^i \tag{6}$$

and the coefficients of eq 6 are given in Table 3.

The path length difference ΔL_0 at the reference state was obtained from repeated calibration measurements carried out in pure water. Additional test measurements were carried out in pure water at temperatures of (323.15, 373.15 and 473.15) K and pressures of (1 or 10, 50, 100, 200 and 300) MPa. The results of this comparison at p = 1 MPa are included in Figure 2, while the data on the isotherms at T/K = 323.15, 373.15 and 473.15 are shown in Figure 3.

The verification measurements at T = 323.15 K are in close agreement with the other data considered in Figure 2. At higher pressures and temperatures, somewhat larger deviations are found but, with one exception, the results remain within the uncertainty of the IAPWS-95 equation, which increases substantially under these conditions. Compared with the high-accuracy experimental data reported by Fujii (relative uncertainty ≈ 0.01 %),[55] we observe very close agreement along the isotherm at T = 323.15 K at pressures up to 200 MPa. The available literature at temperatures between T = (373.15 and 473.15) K is limited but, compared with Aleksandrov and Larkin[56] (relative uncertainty ≤ 0.02 %) and Lin and Trusler[50] (relative uncertainty ≤ 0.04 %), the present results are lower by between (0.01 and 0.10) %.

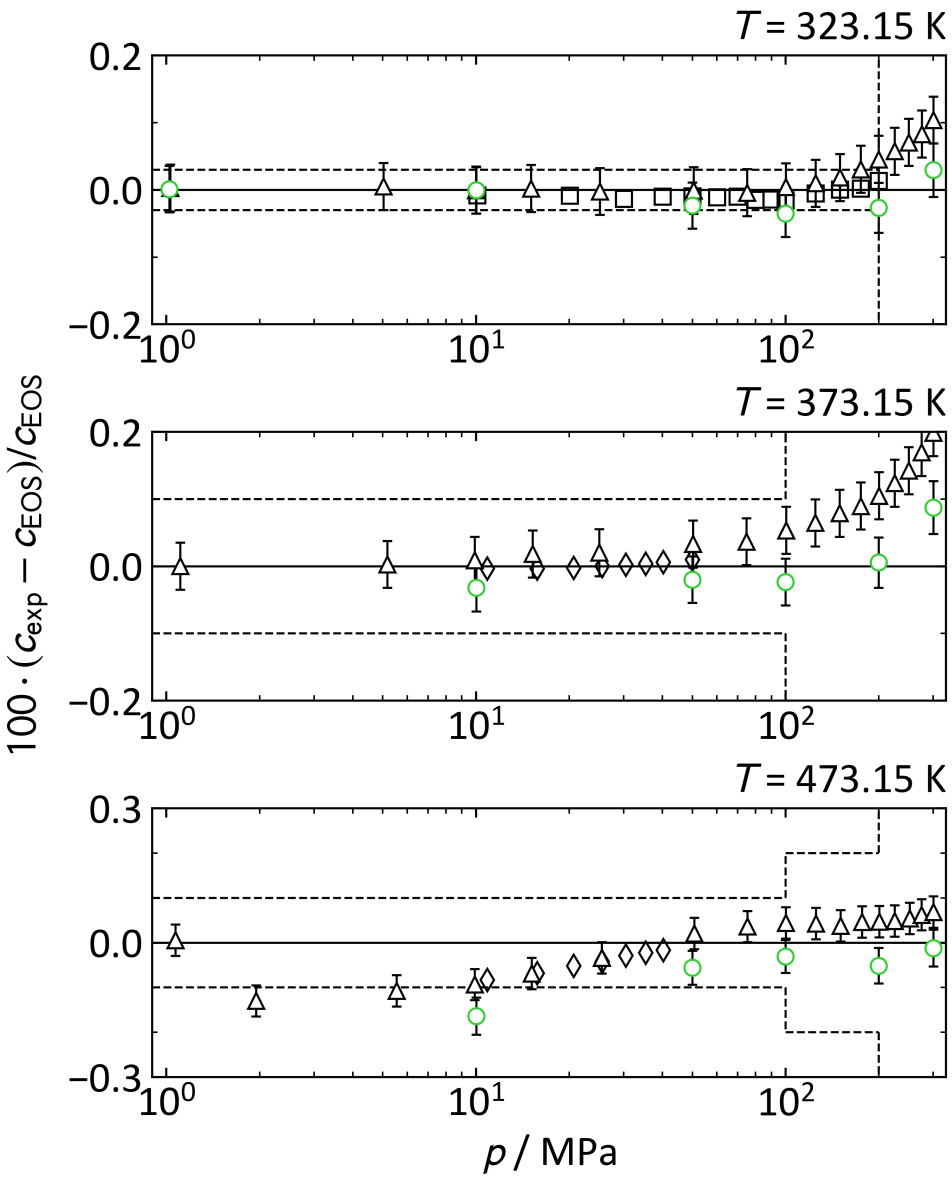

Figure 3. Relative deviations of experimental speeds of sound in pure water c_{exp} (measured at ICL) from values c_{EOS} calculated with the equation of state of Wagner and Pruß[46] plotted versus pressure at T = (323.15 K, 373.15 K and 473.15) K: ○, this work; △, Lin and Trusler;[50] □, Fujii;[55] ◇, Aleksandrov and Larkin.[56] Error bars (shown only where larger than the plotting symbols) represent 95% confidence intervals. Dashed lines represent the uncertainty limits of the equation of state.

2.2 Experimental material. The samples used in this work are detailed in Table 4. Both samples of n-pentane were anhydrous material supplied by Sigma Aldrich with a stated mass fraction of

water of < 0.001%. The purity of both samples was investigated by gas chromatography with flame ionization detection and was found to be 99.8 mass%. At RUB, the impurities present were quantified by gas chromatography with a flame ionization detector and further identified by a comparison with a reference chromatogram of NIST. At ICL, gas chromatography-mass spectrometry (GC-MS) was also used to identify the impurities present and a Coulometric Karl Fischer Titrator (Mettler Toledo C20), with a sensitivity of 1 ppm, was used to test for water but none was detected. Prior to use, n-pentane was transferred into a stainless-steel bottle (at RUB this was done in a glove box filled with dry nitrogen) and degassed by repeated cycles of freezing in liquid nitrogen and evacuation.

Table 4. Description of chemical samples used at RUB and ICL, where w is mass fraction and ρ_e is electrical resistivity.

Chemical name	CAS number	Source	Purity as supplied	Purification method	Final Purity	Analytical method [c]
Water [a]	7732-18	Sigma-Aldrich DE	0.999997	Freeze-thaw		
Water [b]	7732-18	Millipore Direct Q		Reverse osmosis	$\rho_e \geq 18$ MΩ·cm	Elec
Pentane [a]	109-66-0	Sigma-Aldrich DE	> 0.990	Freeze-thaw	$w = 0.998$	GC [d]
Pentane [b]	109-66-0	Sigma-Aldrich UK	> 0.990	Freeze-thaw	$w = 0.998$	GC, KF [e]

[a] Sample used at Ruhr University Bochum
[b] Sample used at Imperial College London
[c] Elec denotes electrical resistivity at $T = 298.15$ K, GC is gas chromatography and KF is Karl-Fisher titration.
[d] Detected impurities: methylbutane (0.17%), cyclopropane (< 0.01%), cyclohexane (< 0.01%), cyclopentane (< 0.01%)
[e] Detected impurities: methylbutane (0.15%), 1-pentene (0.01%) and 1,2 dimethylcyclopropane (< 0.01%)

2.3 Experimental procedure. The procedures used in the two laboratories were essentially identical. The apparatus was initially evacuated thoroughly to remove impurities, and the thermostat bath was set to a low temperature. Next, the sample cylinder containing the pentane was warmed to raise its vapor pressure, and material was transferred into the pressure vessel where it condensed. The hand pump was then used to raise pressure, and the system was left to equilibrate before measurements began.

Measurements were carried out along isotherms, starting at the lowest temperature. At RUB, the measurements were conducted over a temperature range from (233.50 to 353.20) K at pressures up to 20 MPa, while at ICL the ranges were (263.15 to 473.15) K with pressures up to 390 MPa.

2.4 Uncertainty analysis. To estimate the uncertainty of the speed of sound, eqs 1 and 2 were combined, and ΔL_0 was eliminated in favour of the time difference Δt_0 measured in the calibration fluid, resulting in the following working equation:

$$c(T,p) = c_0 \frac{(\Delta t_0 + \tau_0)}{(\Delta t + \tau)} \left[1 + \alpha (T - T_0) - \frac{\beta}{3} (p - p_0) \right] \tag{7}$$

Neglecting the very-small diffraction terms for the uncertainty analysis only, the square of the standard uncertainty of the speed of sound is given according to eq 8:

$$\begin{aligned} u^2(c) &= \left[\left(\frac{\partial c}{\partial c_0} \right) u(c_0) \right]^2 + \left[\left(\frac{\partial c}{\partial \Delta t_0} \right) u(\Delta t_0) \right]^2 + \left[\left(\frac{\partial c}{\partial \Delta t} \right) u(\Delta t) \right]^2 + \left[\left(\frac{\partial c}{\partial \alpha} \right) u(\alpha) \right]^2 + \left[\left(\frac{\partial c}{\partial \beta} \right) u(\beta) \right]^2 \\ &= \left[\left(\frac{c}{c_0} \right) u(c_0) \right]^2 + \left[\left(\frac{c}{\Delta t_0} \right) u(\Delta t_0) \right]^2 + \left[\left(\frac{c}{\Delta t} \right) u(\Delta t) \right]^2 + \left[\left(\frac{c_0 \Delta t_0 (T - T_0)}{\Delta t} \right) u(\alpha) \right]^2 + \left[\left(\frac{-c_0 \Delta t_0 (p - p_0)}{3 \Delta t} \right) u(\beta) \right]^2 \end{aligned} \tag{8}$$

The overall expanded combined uncertainty $U_c(c)$ with a coverage factor k is then given by:

$$U_c(c) = k \sqrt{u^2(c) + \left[(\partial c / \partial p)_T \, u(p) \right]^2 + \left[(\partial c / \partial T)_p \, u(T) \right]^2 + u^2(c(w))} \tag{9}$$

This equation includes a term $u(c(w))$, which represents the standard uncertainty of the sound speed associated with impurities in the sample. Since we have applied no corrections for the presence of impurities, this uncertainty term should account for the full influence of the impurities present. In order to quantify this influence, a sensitivity analysis was carried out using the mixture model available in the REFPROP software.[11] Considering first methylbutane, the principal impurity identified in Table 4 with a mass fraction $w \leq 0.0017$, the estimate changes Δc from the speed of sound in pure pentane falls in the interval $-0.09 \leq \Delta c/(\mathrm{m \cdot s^{-1}}) \leq 0.05$, fractionally $-0.010\% \leq \Delta c/c \leq 0.002\%$. Water as an impurity with $w \leq 1 \cdot 10^{-5}$ would have approximately the same effect, while the other impurities identified in Table 4 would have, at the indicated mass fractions, even smaller effects. For purposes of estimating the uncertainty we set $u^2(c(w)) = (\Delta c)^2 / \sqrt{3}$ with Δc evaluated for the methylbutane impurity at the measured mass fractions reported in Table 4.

The uncertainty budget for sound speed is exemplified in Table 5 for the case of the median temperature and pressure employed in each laboratory. At RUB, the speed of sound $c = 1073\ \mathrm{m \cdot s^{-1}}$ at $T = 293.20\ \mathrm{K}$ and $p = 5\ \mathrm{MPa}$ has an expanded combined uncertainty of $0.168\ \mathrm{m \cdot s^{-1}}$ with a coverage factor $k = 2$, which corresponds to a relative expanded combined uncertainty of 0.016%. At ICL, the speed of sound $c = 1756\ \mathrm{m \cdot s^{-1}}$ at $T = 373.15\ \mathrm{K}$ and $p = 210\ \mathrm{MPa}$ has an expanded combined uncertainty of $0.92\ \mathrm{m \cdot s^{-1}}$ with a coverage factor $k = 2$, which corresponds to a relative expanded combined uncertainty of 0.052%. Over the entire region investigated, $u(c)/c$ is roughly constant at about 0.02%; however, the terms associated with the derivatives of c with respect to T and, especially, p vary strongly, and we find that $U(c)$ varies between (0.16 and 1.40) $\mathrm{m \cdot s^{-1}}$. The corresponding overall relative expanded combined uncertainty ($k = 2$) of the data ranges from 0.015% to 0.18%. For the ICL data, pressure uncertainty is the dominant factor in the overall combined uncertainty at $p \leq 30\ \mathrm{MPa}$.

Table 5. Uncertainty budget for speed of sound measurements conducted at RUB (upper part) and ICL (lower part) at the median state point, where T is temperature, p is pressure, c is sound speed, Δt is time difference, α is the mean isobaric expansivity, β is the mean isothermal compressibility, w is mass fraction and subscript 0 refers to calibration measurements in pure water. Sensitivity coefficients associated with temperature and pressure were estimated from the equation of state of Span and Wagner.[5]

Quantity	Value	Standard uncertainty	Sensitivity coefficient	Uncertainty Contribution
c_0	1482.52 $m \cdot s^{-1}$	0.07 $m \cdot s^{-1}$	0.724	0.054 $m \cdot s^{-1}$
Δt_0	13.32385 μs	0.00017 μs	81 $m \cdot s^{-1} \cdot \mu s^{-1}$	0.014 $m \cdot s^{-1}$
Δt	18.40250 μs	0.00024 μs	58 $m \cdot s^{-1} \cdot \mu s^{-1}$	0.014 $m \cdot s^{-1}$
α	8.37×10^{-6} K^{-1}	4.18×10^{-7} K^{-1}	3.26×10^{-1} $m \cdot s^{-1} \cdot K$	0.001×10^{-4} $m \cdot s^{-1}$
β	2.04×10^{-6} MPa^{-1}	1.02×10^{-7} MPa^{-1}	1.76×10^{3} $m \cdot s^{-1} \cdot MPa$	0.018×10^{-2} $m \cdot s^{-1}$
T	293.202 K	0.004 K	4.60 $m \cdot s^{-1} \cdot K^{-1}$	0.020 $m \cdot s^{-1}$
p	5.0184 MPa	0.0024 MPa	8.54 $m \cdot s^{-1} \cdot MPa^{-1}$	0.020 $m \cdot s^{-1}$
$c(w)$	1073.347 $m \cdot s^{-1}$	0.055 $m \cdot s^{-1}$	1	0.055 $m \cdot s^{-1}$
			Combined expanded uncertainty ($k = 2$) at RUB:	0.168 $m \cdot s^{-1}$
c_0	1498.21 $m \cdot s^{-1}$	0.24 $m \cdot s^{-1}$	1.172	0.282 $m \cdot s^{-1}$
Δt_0	13.3493 μs	0.0003 μs	132 $m \cdot s^{-1} \cdot \mu s^{-1}$	0.040 $m \cdot s^{-1}$
Δt	11.3820 μs	0.0003 μs	154 $m \cdot s^{-1} \cdot \mu s^{-1}$	0.047 $m \cdot s^{-1}$
α	1.3×10^{-6} K^{-1}	0.1×10^{-6} K^{-1}	1.3×10^{5} $m \cdot s^{-1} \cdot K$	0.013 $m \cdot s^{-1}$
β	9.04×10^{-6} MPa^{-1}	0.09×10^{-6} MPa^{-1}	1.2×10^{5} $m \cdot s^{-1} \cdot MPa$	0.011 $m \cdot s^{-1}$
T	373.150 K	0.015 K	1.89 $m \cdot s^{-1} \cdot K^{-1}$	0.028 $m \cdot s^{-1}$
p	210.00 MPa	0.13 MPa	2.85 $m \cdot s^{-1} \cdot MPa^{-1}$	0.359 $m \cdot s^{-1}$
$c(w)$	1756.225 $m \cdot s^{-1}$	0.006 $m \cdot s^{-1}$	1	0.006 $m \cdot s^{-1}$
			Combined expanded uncertainty ($k = 2$) at ICL:	0.92 $m \cdot s^{-1}$

3 RESULTS

The speed of sound in n-pentane was measured at seven or eight (T, p) state points on each of seven isotherms at RUB (see Table 6) and at 11 to 14 state points on each of 11 isotherms at ICL (see Table 7), leading to a total of 197 (p, c, T) data. The results of the measurements, plotted as speed of sound versus pressure, are shown in Figure 4 (RUB) and Figure 5 (ICL), respectively. It is noted that the speed of sound increases with increasing pressure and decreasing temperature. The speeds of sound in n-pentane, measured in this work, vary from 724 $m \cdot s^{-1}$ (T = 473.15 K and p = 30 MPa) to 2332 $m \cdot s^{-1}$ at (T = 283.15 K and p = 390 MPa).

Table 6. Speed of sound c_{exp} and expanded uncertainties $U(c)$ (k = 2) at temperatures T and pressures p measured at RUB.[a]

T / K	p / MPa	c_{exp} / $m \cdot s^{-1}$	$U(c)$ / $m \cdot s^{-1}$	T / K	p / MPa	c_{exp} / $m \cdot s^{-1}$	$U(c)$ / $m \cdot s^{-1}$
233.512	20.003	1442.701	0.190	293.202	5.018	1073.356	0.169
233.512	15.011	1416.020	0.191	293.202	3.515	1060.341	0.169
233.512	10.008	1387.981	0.192	293.202	2.010	1046.996	0.170
233.513	5.011	1358.632	0.189	293.204	0.509	1033.248	0.171
233.512	3.508	1349.518	0.188	293.204	0.156	1029.941	0.171
233.508	2.010	1340.247	0.187	313.206	20.013	1108.625	0.160
233.521	0.507	1330.856	0.186	313.207	15.034	1070.101	0.160
233.508	0.154	1328.590	0.186	313.206	10.014	1028.035	0.161
253.260	19.991	1354.594	0.182	313.206	5.007	982.024	0.163
253.259	15.043	1325.516	0.183	313.206	3.512	967.345	0.164
253.258	10.064	1294.710	0.184	313.206	2.007	952.074	0.165
253.258	5.013	1261.595	0.185	313.207	0.508	936.290	0.166
253.258	3.510	1251.375	0.186	313.206	0.154	932.459	0.163
253.260	2.007	1240.925	0.186	333.208	20.003	1033.135	0.158
253.260	0.509	1230.328	0.187	333.208	15.010	990.848	0.158
253.259	0.156	1227.794	0.175	333.208	10.011	944.401	0.159
273.209	20.041	1269.658	0.174	333.208	5.005	892.477	0.162
273.209	15.005	1237.209	0.174	333.208	3.511	875.672	0.163
273.209	10.018	1203.043	0.175	333.207	2.001	857.973	0.164
273.209	5.028	1166.581	0.177	333.208	0.505	839.616	0.166
273.209	3.516	1155.013	0.177	353.208	20.025	961.467	0.161

T / K	p / MPa	c_{exp} / m·s^{-1}	$U(c)$ / m·s^{-1}	T / K	p / MPa	c_{exp} / m·s^{-1}	$U(c)$ / m·s^{-1}
273.209	2.018	1143.249	0.178	353.207	15.007	914.984	0.162
273.209	0.509	1131.179	0.179	353.207	10.011	863.415	0.163
273.209	0.155	1128.315	0.179	353.207	5.010	804.556	0.167
293.202	20.003	1187.349	0.166	353.207	3.505	784.952	0.169
293.202	15.045	1152.316	0.166	353.207	2.008	764.348	0.171
293.202	10.019	1114.271	0.167	353.206	0.506	742.399	0.174

[a] Standard uncertainties are $u(T) = 0.004$ K, $u(p) = 0.0024$ MPa

Table 7. Speed of sound c_{exp} and expanded uncertainties $U(c)$ ($k = 2$) at temperatures T and pressures p measured at ICL.[a]

T / K	p / MPa	c_{exp} / m·s^{-1}	$U(c)$ / m·s^{-1}	T / K	p / MPa	c_{exp} / m·s^{-1}	$U(c)$ / m·s^{-1}
263.15	1.02	1183.66	0.86	348.15	240.06	1883.05	0.97
263.15	30.03	1368.22	0.71	348.15	270.07	1957.00	1.02
263.15	60.03	1514.87	0.67	348.15	300.08	2026.22	1.06
263.15	90.04	1636.54	0.68	348.15	330.08	2090.99	1.10
263.15	120.04	1742.08	0.75	348.15	360.08	2152.35	1.14
263.15	150.05	1835.54	0.81	348.15	390.09	2210.95	1.17
263.15	180.05	1920.69	0.87	373.15	30.03	979.82	0.86
263.15	210.06	1998.78	0.92	373.15	60.03	1180.90	0.69
263.15	240.06	2071.18	0.97	373.15	90.04	1333.93	0.66
263.15	270.07	2139.00	1.02	373.15	120.04	1460.70	0.74
263.15	300.07	2202.51	1.06	373.15	150.05	1570.39	0.81
273.15	1.03	1134.08	0.89	373.15	180.05	1667.87	0.87
273.15	30.03	1328.08	0.72	373.15	210.06	1756.11	0.92
273.15	60.03	1479.76	0.67	373.15	240.06	1836.82	0.97
273.15	90.04	1604.61	0.68	373.15	270.07	1911.90	1.02
273.15	120.04	1711.86	0.75	373.15	300.07	1981.79	1.06
273.15	150.05	1807.28	0.81	373.15	330.08	2048.24	1.10
273.15	180.05	1893.63	0.87	373.15	360.08	2110.47	1.14
273.15	210.06	1972.96	0.92	373.15	390.09	2169.64	1.18
273.15	240.06	2046.43	0.97	398.15	30.03	907.14	0.91
273.15	270.07	2114.88	1.02	398.15	60.03	1120.24	0.70
273.15	300.07	2179.60	1.06	398.15	90.04	1279.20	0.66
283.15	1.02	1085.38	0.93	398.15	120.04	1409.82	0.74
283.15	30.02	1289.19	0.73	398.15	150.05	1522.25	0.81
283.15	60.03	1445.81	0.67	398.15	180.06	1621.50	0.87

T / K	p / MPa	c_{exp} / m·s^{-1}	$U(c)$ / m·s^{-1}	T / K	p / MPa	c_{exp} / m·s^{-1}	$U(c)$ / m·s^{-1}
283.15	90.04	1573.65	0.67	398.15	210.06	1711.43	0.92
283.15	120.04	1683.44	0.75	398.15	240.06	1793.82	0.97
283.15	150.05	1780.69	0.81	398.15	270.07	1870.11	1.02
283.15	180.05	1868.15	0.87	398.15	300.07	1941.29	1.06
283.15	210.05	1948.39	0.92	398.15	330.08	2008.27	1.10
283.15	240.06	2023.11	0.97	398.15	360.08	2071.53	1.14
283.15	270.07	2092.20	1.02	398.15	390.09	2131.51	1.18
283.15	300.09	2157.17	1.06	423.15	30.03	840.13	0.96
283.15	330.07	2218.78	1.10	423.15	60.03	1064.72	0.71
283.15	360.08	2277.23	1.14	423.15	90.04	1228.76	0.66
283.15	390.09	2332.93	1.17	423.15	120.04	1362.77	0.74
298.15	1.03	1012.42	1.01	423.15	150.04	1477.67	0.81
298.15	30.02	1232.45	0.75	423.15	180.05	1579.06	0.87
298.15	60.03	1396.48	0.67	423.15	210.06	1670.55	0.92
298.15	90.04	1528.91	0.67	423.15	240.06	1754.24	0.97
298.15	120.04	1641.85	0.74	423.15	270.07	1831.52	1.02
298.15	150.04	1741.41	0.81	423.15	300.07	1903.58	1.06
298.15	180.05	1830.87	0.87	423.15	330.08	1971.27	1.10
298.15	210.06	1912.66	0.92	423.15	360.08	2035.32	1.14
298.15	240.06	1988.41	0.97	423.15	390.09	2095.85	1.18
298.15	270.07	2059.19	1.02	448.15	30.03	779.25	1.01
298.15	300.07	2125.06	1.06	448.15	60.03	1014.16	0.72
298.15	330.07	2187.50	1.10	448.15	90.03	1183.45	0.67
298.15	360.09	2246.77	1.14	448.15	120.04	1320.38	0.74
298.15	390.09	2303.12	1.17	448.15	150.05	1437.54	0.81
323.15	1.02	893.41	1.17	448.15	180.05	1540.63	0.87
323.15	30.03	1142.57	0.78	448.15	210.06	1633.25	0.93
323.15	60.03	1318.97	0.68	448.15	240.06	1717.91	0.98
323.15	90.04	1458.72	0.67	448.15	270.07	1796.18	1.02
323.15	120.04	1576.59	0.74	448.15	300.07	1868.95	1.06
323.15	150.05	1679.77	0.81	448.15	330.08	1937.37	1.10
323.15	180.05	1772.17	0.87	448.15	360.08	2001.83	1.14
323.15	210.06	1856.15	0.92	448.15	390.09	2062.94	1.18
323.15	240.06	1933.81	0.97	473.15	30.03	723.54	1.06
323.15	270.07	2006.06	1.02	473.15	60.03	968.08	0.73
323.15	300.07	2073.80	1.06	473.15	90.04	1141.66	0.67
323.15	330.08	2137.21	1.10	473.15	120.04	1281.18	0.75
323.15	360.08	2197.80	1.14	473.15	150.05	1400.26	0.81
323.15	390.09	2255.18	1.17	473.15	180.05	1504.64	0.87
348.15	1.02	773.00	1.41	473.15	210.06	1598.54	0.93

$\frac{T}{\mathrm{K}}$	$\frac{p}{\mathrm{MPa}}$	$\frac{c_{\mathrm{exp}}}{\mathrm{m \cdot s^{-1}}}$	$\frac{U(c)}{\mathrm{m \cdot s^{-1}}}$	$\frac{T}{\mathrm{K}}$	$\frac{p}{\mathrm{MPa}}$	$\frac{c_{\mathrm{exp}}}{\mathrm{m \cdot s^{-1}}}$	$\frac{U(c)}{\mathrm{m \cdot s^{-1}}}$
348.15	30.03	1057.91	0.82	473.15	240.07	1684.27	0.98
348.15	60.03	1246.87	0.68	473.15	270.07	1763.19	1.02
348.15	90.04	1393.52	0.66	473.15	300.07	1836.82	1.06
348.15	120.04	1515.86	0.74	473.15	330.08	1905.79	1.10
348.15	150.05	1622.36	0.81	473.15	360.09	1970.67	1.14
348.15	180.05	1717.53	0.87	473.15	390.10	2032.37	1.18
348.15	210.06	1803.78	0.92				

[a] Standard uncertainties are $u(T) = 0.015$ K, $u(p) = \mathrm{Max}(0.05\ \mathrm{MPa}, 0.0006 \cdot p)$

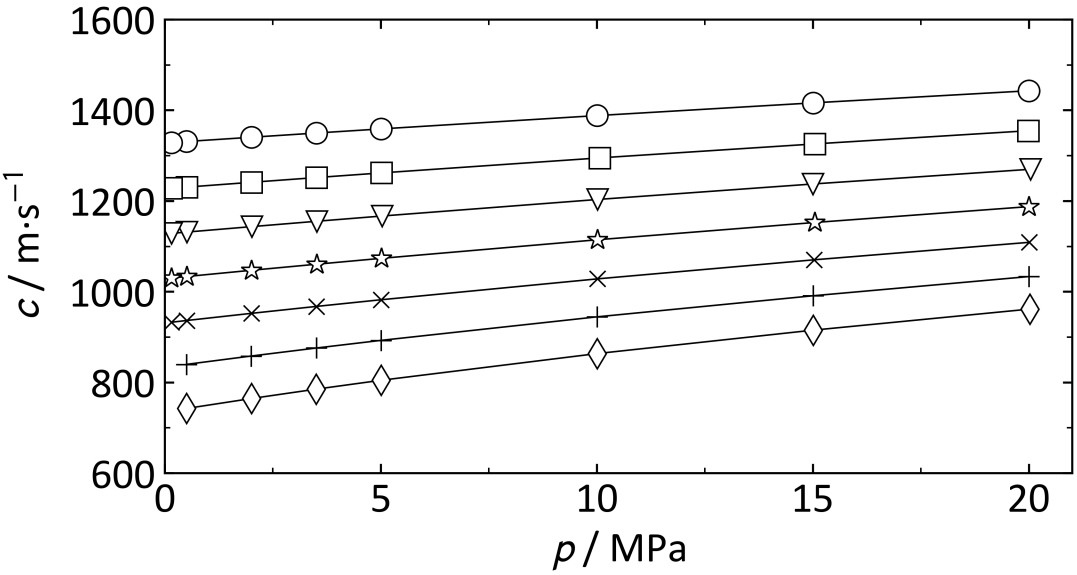

Figure 4. Results of the speed of sound measurements in n-pentane. Absolute speeds of sound c_{exp} measured at RUB are plotted versus pressure. ○, 233.50 K; □, 253.26 K; ▽, 273.21 K; ☆, 293.20 K; ×, 313.21 K; +, 333.21 K; ◇, 353.21 K. Lines are shown only to guide the eye.

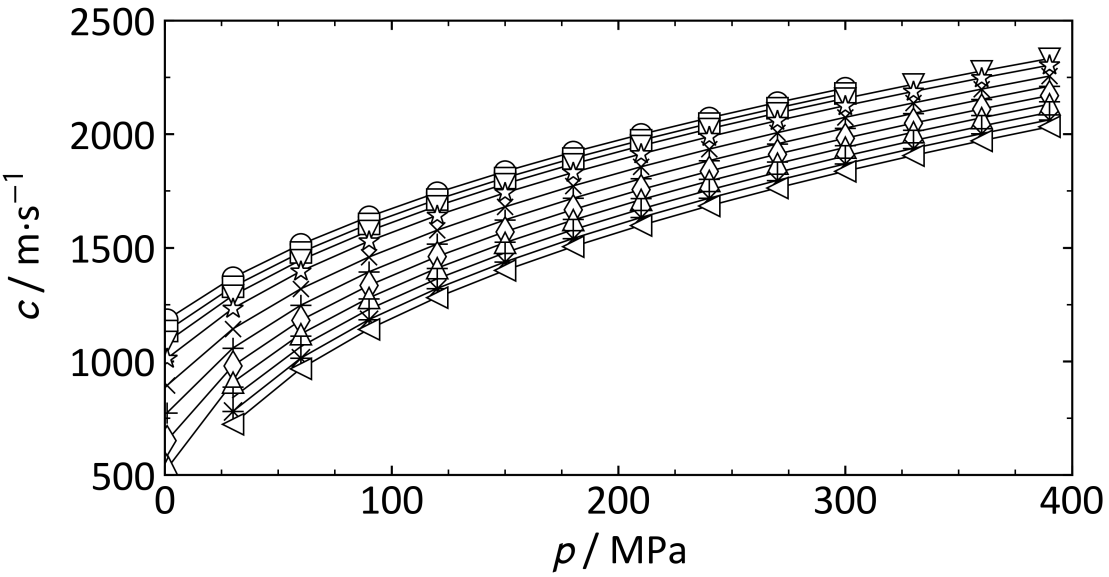

Figure 5. Results of the speed of sound measurements in n-pentane. Absolute speeds of sound c_{exp} measured at ICL are plotted versus pressure. ○, 263.15 K; □, 273.15 K; ▽, 283.15 K; ☆, 298.15 K; ×, 323.15 K; +, 348.15 K; ◇, 373.15 K; △, 398.15 K; ⊤, 423.15 K; ✳, 448.15 K; ◁, 473.15 K. Lines are shown only to guide the eye.

4 DISCUSSION

Figures 6 and 7 compare the speeds of sound data measured at RUB and ICL along isotherms with the equation of state of Thol et al.[6] as reference (zero line). Deviations of the speeds of sound calculated from the equation of state of Span and Wagner[5] are also illustrated as dashed curves. It should be noted that the RUB results were already considered in the development of the equation of state of Thol et al.[6] In Figure 6, one can observe that the data from RUB are represented essentially within experimental uncertainty, except on the lowest isotherm where they deviate by approximately +0.11%. Only the lowest pressures studied on the isotherms at $T \leq 348.15$ K at ICL overlap with the RUB data set. In this overlapping region, the ICL data are, on average, 0.13% lower than both the RUB data and the preliminary equation of state. These differences are slightly

larger than the combined uncertainty which, for the ICL data, is limited at these low pressures by the uncertainty of the pressure transducer.

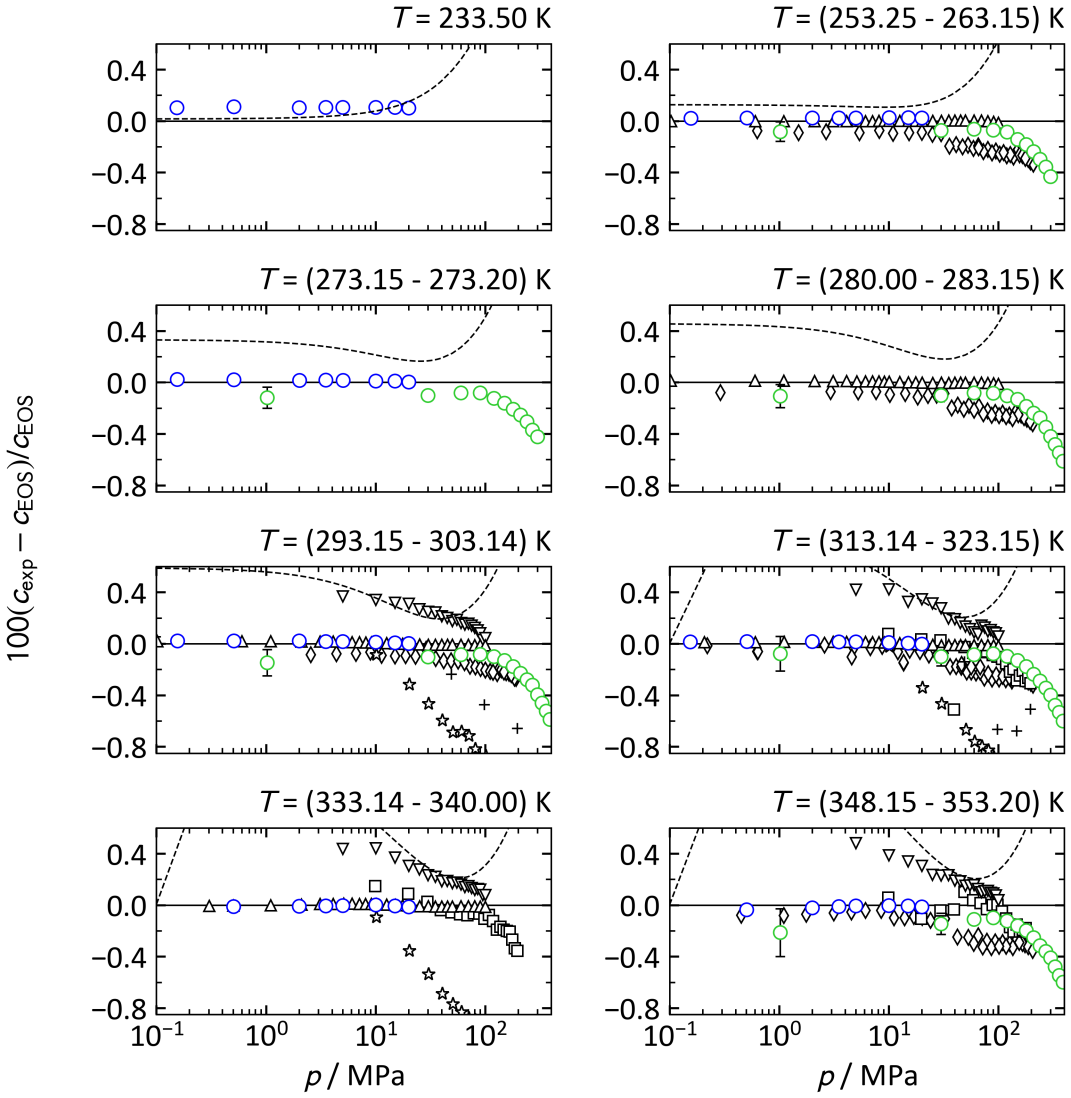

Figure 6. Results of the speed of sound measurements in n-pentane. Relative deviations of the experimental speeds of sound c_{exp} from values c_{EOS} calculated with the equation of state of Thol et al.[6] are plotted versus pressure: ○, this work at RUB; ○, this work at ICL; △, El Hawary et al.;[9] ◇, Lainez et al.;[20] □, Otpushchennikov et al.;[27] +,Belinskii and Ikramov;[12] ▽, Ding et al.;[15] ☆, Kiryakov and Otpushchennikov;[19] ---, EOS of Span and Wagner.[5]

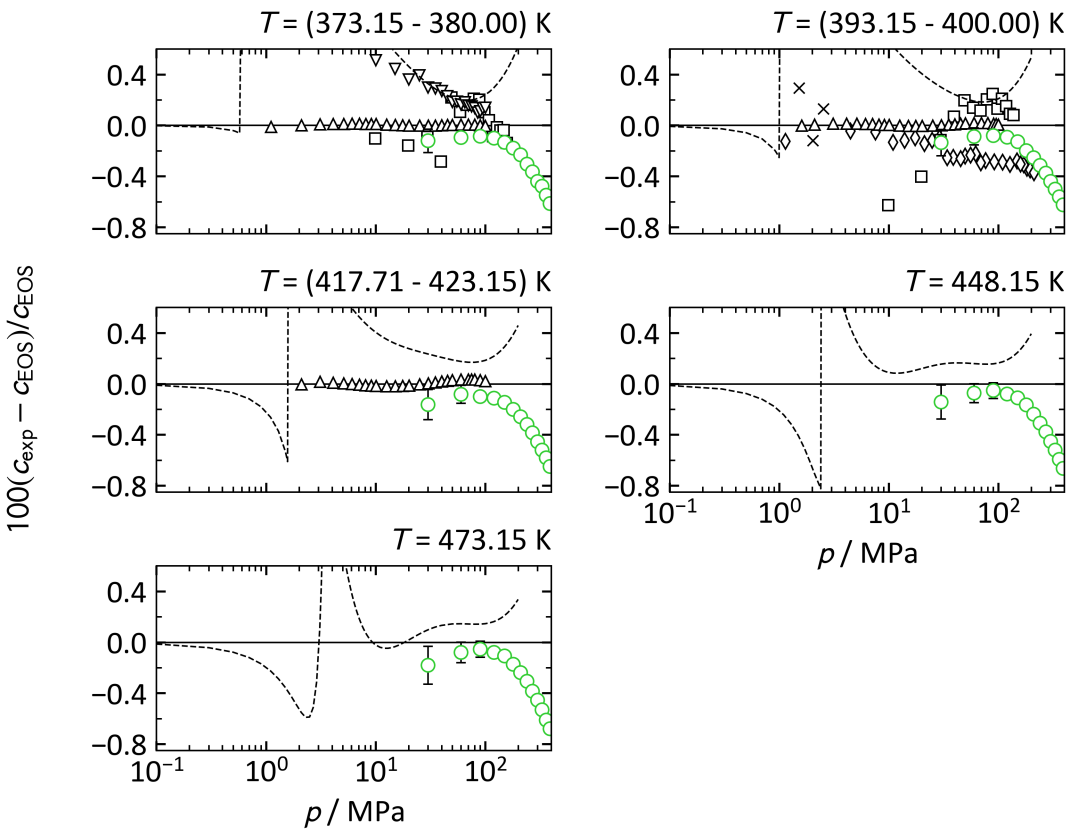

Figure 7. Results of the speed of sound measurement in n-pentane. Relative deviations of the experimental speeds of sound c_{exp} from values c_{EOS} calculated with the equation of state of Thol et al.[6] are plotted versus pressure: ○, this work at ICL; △, El Hawary et al.;[9] ◇, Lainez et al.;[20] □, Otpushchennikov et al.;[27] ▽, Ding et al.;[15] ×, Ismagilov et al.;[18] ---, EOS of Span and Wagner.[5]

As seen in Figures 6 and 7, the ICL data at high pressures, especially above 100 MPa, are not in agreement with the equation of state over the entire temperature range; the worst deviation, at the highest temperature and pressure, is -0.68%. These deviations cannot be attributed with certainty to either experimental error or to imperfections in the equation of state. However, the equation of Thol et al.[6] is at least much closer to the experimental data than the one of Span and Wagner.[5]

Figure 6 and 7 also show relative deviations of literature data from the equation of state of Thol et al.[6] As mentioned above, the data set of El Hawary et al.[9] was also used for the development of this equation of state and agree best with the data reported here. At temperatures between (273.21 and 353.21) K, the data of El Hawary et al. agree to within ±0.015% with our data measured at RUB, while a systematically offset of 0.05% can be observed at 253.26 K. The data of El Hawary et al. also differs by up to 0.06% at lower temperatures and by up to 0.17% at temperatures near 420.15 K from our data measured at ICL. The speed of sound reported by Ding et al.[15] deviate from our results by about +0.5% at the lowest pressures, but the deviations diminish with increasing pressure to around 0.1% at p = 100 MPa. Furthermore, the data set of Lainez et al.[20] is in good agreement with our data measured at ICL at pressures up to 30 MPa. Starting at a pressure slightly above 30 MPa, the data of Lainez et al. exhibit larger deviations amounting to about -0.25% at p = 100 MPa; this might be explained by a change of their pressure sensor at p = 34 MPa. However, with further increase in pressure, these deviation reduce and the data of Lainez et al. agree with our results to within about 0.05% at pressures near 200 MPa. Moreover, our data agree with the data of Otpushchennikov et al.[27] at temperatures between (313.21 and 353.21) K and pressures ≥ 40 MPa within ±0.1%. In the overlapping pressure region on higher isotherms at (373.15 and 393.15) K, the the data of Otpushchennikov et al.[27] differs by up to (0.30 or 0.33)%, respectively. The only other speeds of sound available at pressures beyond 200 MPa are the data of Belinskii and Ikramov[12] in the temperature range from (293.15 to 313.15) K. These data deviate from our measurements by -0.5 % at T = 293.15 K and p = 400 MPa and show large negative deviations from the equation of state of Thol et al.,[6] reaching -3.7% at T = 313.15 K and p = 785 MPa.

5 CONCLUSION

We report speeds of sound measured in samples of high-purity n-pentane in two different laboratories operating in complementary ranges of temperature and pressure. The overall relative expanded combined uncertainty ($k = 2$) of the data ranges from 0.015% to 0.18%. In the region of overlap, the two data sets agree to within an average of 0.13%. The new data deviate from the equation of state of Span and Wagner[5] by up to 2% but agree with the new equation of state of Thol et al.[10] to within 0.7% and, at $p \leq 20$ MPa, to within 0.1% or better. The experimental data reported here have been partly used for the development of this equation of state and could primarily confirm the simultaneously and independently obtained data set of El Hawary et al.,[9] which was also considered as primary data.

ACKNOWLEDGEMENTS

We thank our colleagues from the group of Prof. Ulf-Peter Apfel (faculty of chemistry and biochemistry at RUB) for making available their glove box for the sample transfer and for supporting us with the GC-analysis of the sample used at RUB.

REFERENCES

(1) Hettiarachchia, H. D. M.; Golubovica, M.; Worek, W. M.; Ikegami, Y. Optimum Design Criteria for an Organic Rankine Cycle Using Low-Temperature Geothermal Heat Sources. *Energy* **2007**, *32*, 1698-1706.

(2) Becken, K.; Graaf, D. d.; Elsner, C.; Hoffmann, G.; Krüger, F.; Martens, K.; Plehn, W.; Sartorius, R., Avoiding Fluorinated Greenhouse Gases - Prospects for Phasing Out. In Federal Environment Agency: Dessau-Roßlau, Germany, 2010.

(3) Pérez-Silva, A.; Odoux, E.; Brat, P.; Ribeyre, F.; Rodriguez-Jimenes, G.; Robles-Olvera, V.; García-Alvarado, M. A.; Günata, Z. GC–MS and GC–Olfactometry Analysis of Aroma Compounds in a Representative Organic Aroma Extract from Cured Vanilla (Vanilla Planifolia G. Jackson) Beans. *Food Chem.* **2006**, *99*, 728-735.

(4) Villalobos, M. A.; Hamielec, A. E.; Wood, P. E. Bulk and Suspension Polymerization of Styrene in the Presence of n-pentane. An Evaluation of Monofunctional and Bifunctional Initiation. *J. Appl. Polym. Sci.* **1993**, *50*, 327-343.

(5) Span, R.; Wagner, W. Equations of State for Technical Applications. II. Results for Nonpolar Fluids. *Int. J. Thermophys.* **2003**, *24*, 41-109.

(6) Thol, M.; Uhde, T.; Richter, M.; Span, R.; Lemmon, E. W. Thermodynamic Properties for Hydrocarbons. I. Fundamental Equation of State for n-pentane. *J. Phys. Chem. Ref. Data* **2020**, *(To be submitted)*.

(7) Lemmon, E. W.; Bell, I. H.; Huber, M. L.; McLinden, M. O. *NIST Standard Reference Database 23: Reference Fluid Thermodynamic and Transport Properties-REFPROP, Version 10.0*, National Institute of Standards and Technology: Gaitherburg, 2018.

(8) Span, R.; Beckmüller, R.; Eckermann, T.; Herrig, S.; Hielscher, S.; Jäger, A.; Neumann, T.; Pohl, S.; Semrau, B.; Thol, M. *TREND. Thermodynamic Reference and Engineering Data 4.0*, Lehrstuhl für Thermodynamik: Ruhr-Universität Bochum: Bochum, Germany, 2019.

(9) El Hawary, A.; Mirzaev, S. Z.; Meier, K. Speed-of-Sound Measurements in Liquid n-Pentane and Isopentane. *J. Chem. Eng. Data* **2020**, *65*, 1243-1263.

(10) Ewing, M. B.; Goodwin, A. R. H.; Trusler, J. P. M. Thermophysical Properties of Alkanes from Speeds of Sound Determined Using a Spherical Resonator 3. n-Pentane. *J. Chem. Thermodyn.* **1989**, *21*, 867-877.

(11) Chávez, M.; Palaclos, J. M.; Tsumura, R. Speed of Sound in Saturated Liquid Normal-Pentane. *J. Chem. Eng. Data* **1982**, *27*, 350-351.

(12) Belinskii, B. A.; Ikramov, S. K. Comprehensive Investigation of Acoustical Parameters, Viscosity, and Density of n-Pentane over a Wide Pressure Interval. *Akust. Zh.* **1973**, *18*, 300-303.

(13) Benson, G. C.; Handa, Y. P. Ultrasonic Speeds and Isentropic Compressibilities for (Decan-1-ol + Normal-Alkane) at 298.15 K. *J. Chem. Thermodyn.* **1981**, *13*, 887-896.

(14) Dalai, B.; Dash, S. K.; Singh, S. K.; Swain, N.; Swain, B. B. Physico-Chemical Properties of Di-(2-Ethylhexyl) Phosphoric Acid with Apolar Solvents from Ultrasonic Studies. *Phys. Chem. Liq.* **2012**, *50*, 242-253.

(15) Ding, Z. S.; Alliez, J.; Boned, C.; Xans, P. Automation of an Ultrasound Velocity Measurement System in High-Pressure Liquids. *Meas. Sci. Technol.* **1997**, *8*, 154-161.

(16) Dixon, H. B.; Greenwood, G. On the Velocity of Sound in Gases and Vapours, and the Ratio of the Specific Heats. *Proc. Roy. Soc. London. A Mat.* **1924**, *105*, 199-220.

(17) Handa, Y. P.; Halpin, C. J.; Benson, G. C. Ultrasonic Speeds and Isentropic Compressibilities for (Hexan-1-ol + Normal-Alkane) at 298.15 K. *J. Chem. Thermodyn.* **1981**, *13*, 875-886.
(18) Ismagilov, R. G.; Ermakov, G. V. Speed of Sound in Superheated Organic Liquids. *High Temperature* **1982**, *20*, 561-566.
(19) Kiryakov, B. S.; Otpushchennikov, N. F. *Issues Kursk Pedag. Inst.* **1971**, 104-112.
(20) Lainez, A.; Zollweg, J. A.; Streett, W. B. Speed-of-Sound Measurements for Liquid n-Pentane and 2,2-Dimethylpropane under Pressure. *J. Chem. Thermodyn.* **1990**, *22*, 937-948.
(21) Melnikov, G. A.; Verveiko, V. N.; Otpushchennikov, N. F. Complex Studies of Elastic and Caloric Properties of Hydrocarbons and Their Halogen-Substituents by the Acoustic Method. *Zh. Fiz. Khim.* **1988**, *62*, 798-800.
(22) Nath, J. Speeds of Sound in and Isentropic Compressibilities of (n-Butanol Plus n-Pentane, or n-Hexane, or n-Heptane, or n-Octane, or 2,2,4-Trimethylpentane, or Carbon Tetrachloride) at T=293.15 K. *J. Chem. Thermodyn.* **1997**, *29*, 853-863.
(23) Nath, J. Speeds of Sound in and Isentropic Compressibilities of (n-Butanol Plus n-Pentane) at T = 298.15 K, and (n-Butanol Plus n-Hexane, or n-Heptane, or n-Octane, or 2,2,4-Trimethylpentane) at T = 303.15 K. *J. Chem. Thermodyn.* **1998**, *30*, 885-895.
(24) Nath, J. Speeds of Sound and Isentropic Compressibilities of (n-Heptanol Plus n-Pentane, or n-Hexane, or n-Heptane, or n-Octane) at T = 303.15 K, and of (n-Heptanol + 2,2,4-Trimethylpentane) at T=293.15 and 303.15 K. *Fluid Phase Equilib.* **2000**, *175*, 63-73.
(25) Nath, J. Speeds of Sound in and Isentropic Compressibilities of (n-Butanol Plus n-Pentane, or n-Hexane, or n-Heptane, or 2,2,4-Trimethylpentane) at T = 288.15 K, (n-Hexanol Plus n-Pentane or n-Hexane) at T = 298.15 K, and (n-Hexanol Plus n-Heptane or n-Octane) at T = 298.15 K and T = 303.15 K. *J. Chem. Thermodyn.* **2002**, *34*, 1857-1872.
(26) Neruchev, Y. A.; Bolotnikov, M. F.; Zotov, V. V. Investigation of Ultrasonic Velocity in Organic Liquids on the Saturation Curve. *High Temperature* **2005**, *43*, 266-309.
(27) Otpushchennikov, N.; Kiryakov, B.; Panin, P. Velocity of Sound and Some Thermodynamic Properties of Liquid n-pentane in a Wide Range of Temperatures and Pressures. *Vyssh. Uchebn. Zaved. Neft Gaz* **1974**, *17*, 73-77.
(28) Rai, R. D.; Shukla, R. K.; Shukla, A. K.; Pandey, J. D. Ultrasonic Speeds and Isentropic Compressibilities of Ternary Liquid-Mixtures at (298.15+/-0.01) K. *J. Chem. Thermodyn.* **1989**, *21*, 125-129.
(29) Richardson, E. G. In *Proceedings of the Joint Conference on Thermodynamic and Transport Properties of Fluids*, London, 1957; Institution of Mechanical Engineers: London, 1957; pp 34-36.
(30) Richardson, E. G.; Tait, R. I. Ratios of Specific Heat and High-Frequency Viscosities in Organic Liquids under Pressure, Derived from Ultrasonic Propagation. *The Philosophical Magazine: A Journal of Theoretical Experimental and Applied Physics* **1957**, *2*, 441-454.
(31) Sachdeva, V. K.; Nanda, V. S. Ultrasonic Wave Velocity in Some Normal Paraffins. *J. Chem. Phys.* **1981**, *75*, 4745-4746.
(32) Schaaffs, W. Investigations on the Velocity of Sound and Constitution. I. The Velocity of Sound in Organic Liquids. *Z. Ph. Chem. (Leipzig)* **1944**, *194*, 28-38.

(33) Shukla, R. K.; Kumar, A.; Shukla, A.; Srivastava, K. Density, Ultrasonic Velocity, Surface Tension, Excess Volume and Viscosity of Quaternary Fluid Solutions. *J. Mol. Liq.* **2008**, *140*, 117-122.
(34) Singh, S.; Yasmin, M.; Shukla, D.; Parveen, S.; Gupta, M. Thermoacoustical Study of Molecular Interactions in Binary Mixtures of Pentane with Methanol and Tert-Butanol. *Phys. Chem. Liq.* **2012**, *50*, 210-221.
(35) Swanson, J. C. Pressure Coefficients of Acoustic Velocity for Nine Organic Liquids. *J. Chem. Phys.* **1934**, *2*, 689-693.
(36) Vyas, V. Ultrasonic Investigation of Effective Debye Temperature in Multi-Component Liquid Systems at 298.15 K. *Phys. Chem. Liq.* **2004**, *42*, 229-236.
(37) Weissler, A.; Del Grosso, V. A. Ultrasonic Investigation of Liquids. VI. Acetylene Derivatives. *JACS* **1950**, *72*, 4209-4210.
(38) Harris, G. R. Transient Field of a Baffled Planar Piston Having an Arbitrary Vibration Amplitude Distribution. *J. Acoust. Soc. Am.* **1981**, *70*, 186-204.
(39) Meier, K.; Kabelac, S. Speed of Sound Instrument for Fluids with Pressures up to 100 MPa. *Rev. Sci. Instrum.* **2006**, *77*.
(40) Gedanitz, H.; Davila, M. J.; Baumhogger, E.; Span, R. An Apparatus for the Determination of Speeds of Sound in Fluids. *J. Chem. Thermodyn.* **2010**, *42*, 478-483.
(41) Wegge, R. Thermodynamic Properties of the (Argon + Carbon Dioxide) System: Instrument Development and Measurements of Density and Speed of Sound. PhD, Ruhr-Universität Bochumn, Bochumn, 2016.
(42) Wegge, R.; Richter, M.; Span, R. Speed of Sound Measurements in Deuterium Oxide (D_2O) over the Temperature Range from (278.2 to 353.2) K at Pressures up to 20 MPa. *Fluid Phase Equilib.* **2016**, *418*, 175-180.
(43) Dubberke, F. H.; Baumhögger, E.; Vrabec, J. Burst Design and Signal Processing for the Speed of Sound Measurement of Fluids with the Pulse-Echo Technique. *Rev. Sci. Instrum.* **2015**, *86*, 054903.
(44) Meier, K. Das Puls-Echo Verfahren für Präzisionsmessungen der Schallgeschwindigkeit in Fluiden. Helmut-Schmidt-University, Hamburg, 2006.
(45) *Verein Deutscher Eisenhüttenleute: Stahl-Eisen-Werkstoffblätter: SEW 310. Table 43.9*. Stahleisen: Düsseldorf, 1997.
(46) Wagner, W.; Pruß, A. The IAPWS Formulation 1995 for the Thermodynamic Properties of Ordinary Water Substance for General and Scientific Use. *J. Phys. Chem. Ref. Data* **2002**, *31*, 387-535.
(47) Del Grosso, V. A.; Mader, C. W. Speed of Sound in Pure Water. *J. Acoust. Soc. Am.* **1972**, *52*, 1442-&.
(48) Fujii, K.; Masui, R. Accurate Measurements of the Sound-Velocity in Pure Water by Combining a Coherent Phase-Detection Technique and a Variable Path-Length Interferometer. *J. Acoust. Soc. Am.* **1993**, *93*, 276-282.
(49) Ball, S. J.; Trusler, J. P. M. Speed of Sound of n-Hexane and n-Hexadecane at Temperatures between 298 and 373 K and Pressures up to 100 MPa. *Int. J. Thermophys.* **2001**, *22*, 427-443.

(50) Lin, C.-W.; Trusler, J. P. M. The Speed of Sound and Derived Thermodynamic Properties of Pure Water at Temperatures between (253 and 473) K and at Pressures up to 400 MPa. *J. Chem. Phys.* **2012**, *136*.
(51) Tay, W. J.; Trusler, J. P. M. Density, Sound Speed and Derived Thermophysical Properties of n-nonane at Temperatures between (283.15 and 473.15) K and at Pressures up to 390 MPa. *J. Chem. Thermodyn.* **2018**, *124*, 107-122.
(52) Al Ghafri, S. Z. S.; Matabishi, E. A.; Trusler, J. P. M.; May, E. F.; Stanwix, P. L. Speed of Sound and Derived Thermodynamic Properties of Para-Xylene at Temperatures between (306 and 448) K and at Pressures up to 66 MPa. *J. Chem. Thermodyn.* **2019**, *135*, 369-381.
(53) Tanji, Y. Thermal Expansion Coefficient and Spontaneous Volume Magnetostriction of Fe-Ni (Fcc) Alloys. *J. Phys. Soc. Jpn.* **1971**, *31*, 1366-1373.
(54) Hausch, G.; Warlimont, H. Single Crystalline Elastic Constants of Ferromagnetic Face Centered Cubic Fe-Ni Invar Alloys. *Acta Metall.* **1973**, *21*, 401-414.
(55) Fujii, K. In *Proceedings of the 12th Symposium on Thermophysical Properties*, 12th Symposium on Thermophysical Properties, Boulder, CO, 1994; Plenum Press, New York: Boulder, CO, 1994; p 19.
(56) Aleksandrov, A. A.; Larkin, D. K. Experimental Study of Speed of Ultrasonic Sound in the Water in a Large Range of Temperatures and Pressures. *Teploenergetiks* **1976**, *23*, 75-78.